ORNL/NUREG/TM-132

Quarterly Progress Report on the Zirconium Metal-Water Oxidation Kinetics Program Sponsored by the NRC Division of Reactor Safety Research for April–June 1977

J. V. Cathcart

Prepared for the U.S. Nuclear Regulatory Commission
Office of Nuclear Regulatory Research
Under Interagency Agreements ERDA 40-551-75 and 40-552-75

OAK RIDGE NATIONAL LABORATORY
OPERATED BY UNION CARBIDE CORPORATION FOR THE ENERGY RESEARCH AND DEVELOPMENT ADMINISTRATION

Printed in the United States of America. Available from
National Technical Information Service
U.S. Department of Commerce
5285 Port Royal Road, Springfield, Virginia 22161
Price: Printed Copy $4.00; Microfiche $3.00

ORNL/NUREG/TM-132
Dist. Category NRC-3

Contract No. W-7405-eng-26

METALS AND CERAMICS DIVISION

QUARTERLY PROGRESS REPORT ON THE ZIRCONIUM METAL-WATER OXIDATION KINETICS PROGRAM SPONSORED BY THE NRC DIVISION OF REACTOR SAFETY RESEARCH FOR APRIL—JUNE 1977

J. V. Cathcart

Manuscript Completed — July 26, 1977

Date Published — August 1977

Prepared for the
U.S. Nuclear Regulatory Commission
Office of Nuclear Regulatory Research
Under Interagency Agreements ERDA 40-551-75 and 40-552-75

OAK RIDGE NATIONAL LABORATORY
Oak Ridge, Tennessee 37830
operated by
UNION CARBIDE CORPORATION
for the
ENERGY RESEARCH AND DEVELOPMENT ADMINISTRATION

CONTENTS

SUMMARY

During the past quarter, scoping tests of the effect of steam pressure [3.45 MPa (500 psi)] on the oxidation of Zircaloy were completed at 900 and 1100°C (1652—2012°F). No effect was observed at 1100°C (2012°F), but at 900°C (1652°F) a significant problem with reproducibility was encountered in relatively long-time experiments. Additional tests in steam at 6.9 MPa (1000 psi) are in progress.

The evaluation of possible effects on oxidation kinetics of hydrogen dissolved in the alpha or beta phases of Zircaloy was completed. Zircaloy was observed to oxidize slightly faster in pure oxygen, i.e., in the complete absence of hydrogen, than in steam. However, this phenomenon was traced to an effect in the oxide alone and was shown to be independent of the presence of dissolved hydrogen in the metals phases of the specimens. It was concluded, therefore, that our previously reported oxidation rate data in steam were unaffected by the hydrogen observed in the oxidized specimens.

Further *in situ* temperature measurement tests were carried out in the MiniZWOK oxidation apparatus. A thermocouple reading of 1064.4 ± 0.3°C (1915.9 ± 0.5°F) was obtained when a specimen was held at the gold point [reference temperature 1064.4°C (1915.9°F)]. A similar experiment involving the α-γ transition temperature for iron yielded a result of 912.7 ± 0.1°C (1674.9 ± 0.2°F) as compared to the reference temperature of 912°C (1673°F). These experiments provided additional support for our previous estimates of maximum temperature uncertainty measurements in the MiniZWOK apparatus.

ZIRCONIUM METAL-WATER OXIDATION KINETICS

J. V. Cathcart

ABSTRACT

Scoping tests of the effect of steam pressure on the oxidation rate of Zircaloy-4 yielded negative results at 1100°C (2012°F) for steam at 3.45 MPa (500 psi); problems with reproducibility were encountered at 900°C (1652°F). Additional experiments in 6.9 MPa (1000 psi) steam are in progress. Measurements of the oxidation rate of Zircaloy-4 specimens in pure oxygen led to the conclusion that hydrogen previously reported present in oxidized specimens had no effect on measured rates of oxidation in steam. Additional *in situ* tests in the MiniZWOK apparatus confirmed the validity of previous estimates of maximum temperature measurement uncertainties.

INTRODUCTION

The ZMWOK program was designed to provide a base data set for the calculation of the reaction kinetics for the high temperature reaction of Zircaloy-4 with steam. Work on this project is now virtually complete. Efforts during the past quarter included studies of the effect of steam pressure on the oxidation of Zircaloy, further evaluation of possible effects of dissolved hydrogen on the oxidation rate of Zircaloy, and additional *in situ* tests of the accuracy of temperature measuring procedures used in the program.

STEAM PRESSURE EFFECTS

R. E. Pawel and J. J. Campbell

We are performing scoping tests to determine the influence of steam pressure on the isothermal oxidation kinetics of Zircaloy-4 PWR tubing. The sets of experiments at 3.45 MPa (500 psi) and at nominal

temperatures of 900 and 1100°C (1652 and 2012°F) are complete. The high-pressure steam oxidation apparatus, SuperZWOK, is presently being modified in order to permit several additional experiments to be conducted at 6.90 MPa (1000 psi) in flowing steam.

Experimental Procedure

The SuperZWOK apparatus permits a Zircaloy-4 tube specimen to be oxidized in flowing, high-pressure steam in a manner similar to that employed in our standard experiments at atmosphere pressure. Basically, the equipment consists of two interconnected autoclaves; one autoclave serves as a boiler while the other houses a radiant heating furnace to heat the specimen through the desired temperature cycle. The flow of steam is controlled at a given pressure by regulating the power to the boiler heater. The apparatus and general experimental procedures have been described in detail in previous Quarterly Reports.[1-3]

Results

Since the last report, nine additional oxidation experiments have been performed in the SuperZWOK apparatus at steam pressures of 3.45 MPa (500 psi). Contrary to the procedure used in previous experiments, the flow of argon used to cool the quad-elliptical heating lamps was eliminated in these more recent tests. This change together with substantial flow of fresh steam obviated the possibility of appreciable steam-argon mixing at the surface of the specimen during the period of isothermal oxidation.

The response of the pressure control valves, with the system operating on steam flow alone, was somewhat sluggish, making control of the specimen temperature more difficult. However, temperature fluctuations about the control point were generally less than ±10°C (±18°F), and we consider the approximation to isothermal oxidation conditions to have been satisfactory in these experiments.

A listing of the phase thickness measurements for all experiments conducted to date at a steam pressure of 3.45 MPa (500 psi) is given

in Tables 1 and 2. Values of the total oxygen consumed by each specimen are also tabulated. These values were calculated on the basis of a model which assumed that all of the oxide was stoichiometric, that a linear oxygen concentration gradient existed in the alpha layer, and that a simplified diffusion calculation accounts adequately for the amount of oxygen in the beta phase. The kinetics of oxide and alpha growth for these sets of specimens are presented in Figs. 1 through 4 where they are compared with the values from the standard MiniZWOK data set obtained for steam oxidation at atmospheric pressure.

The comparison of the MiniZWOK (atmospheric pressure) and SuperZWOK (3.45 MPa) data for oxidation at 1101°C (2014°F) given in Figs. 1 and 2 shows very good agreement in the phase layer thicknesses. Thus, at least for the time and pressure range encompassed by these tests, no measurable pressure effect is evident from the data.

At 905°C (1661°F), as presented in Figs. 3 and 4, the equivalence of the results is less evident. At least part of the problem is associated with the comparatively large scatter in oxide thickness measurements for the 3.45 MPa experiments. While the short-time results and some of the long-time results compare well with the standard (atmospheric pressure) data, several long-time experiments yielded greater oxide thicknesses. The alpha layer growth rates, on the other hand, appear to be essentially identical.

Metallographic examination of these specimens revealed an interesting and significant difference in the appearance of the oxide on specimens with relatively thick oxide layers. Oxide layers from the standard MiniZWOK experiments were examined in both bright-field and in polarized light illumination and compared to those from the high pressure tests. While little difference in the appearance of the oxide layers was evident in bright-field illumination, a bright band of material could be observed in polarized light on the outer portion for several of the SuperZWOK specimens. The specimens exhibiting a significant proportion of this bright-appearing oxide were the longer time experiments, and the thickest oxides noted in Fig. 3 seemed to be the most affected. An

Table 1. Steam Oxidation of Sandvik Zircaloy-4 PWR Tubing at 905°C (1661°F), 3.45 MPa (500 psi)

Expt. No.	Time (s)	Oxide Layer (μm)	Alpha Layer (μm)	Total Oxygen (mg/cm^2)
Z-12	430	10.9	8.3	1.851
Z-14	392	11.8	10	2.03
Z-16	530	12.2	10.7	2.107
Z-18	896	16.7	15.3	2.902
Z-19	103	6.5	5.6	1.12
Z-29	1111	13.8	13.6	2.422
Z-36	1435	17.2	17.7	3.039
Z-40	1254	20	14.6	3.38
Z-44	1069	18.5	13.6	3.129
Z-45	2235	15.5	20	2.842
Z-46	753	16.9	10.3	2.805
Z-48	2711	22.5	20.5	3.908
Z-50	1923	21.9	20.2	3.809
Z-17[a]	410	11.3	12	2.005

[a]Experiment conducted at .14 MPa (20 psi).

Table 2. Steam Oxidation of Sandvik Zircaloy-4 PWR Tubing at 1101°C (2014°F), 3.45 MPa (500 psi)

Expt. No.	Time (s)	Oxide Layer (μm)	Alpha Layer (μm)	Total Oxygen (mg/cm^2)
Z-23	121	22.7	23.2	4.43
Z-24	198	28.9	29.4	5.635
Z-30	173	26.4	21.1	4.994
Z-34	416	36.9	38.6	7.304
Z-35	532	45.5	45.2	8.87
Z-41	35	13.3	9.7	2.467
Z-42	344	38.8	34.5	7.413
Z-43	294	36.4	33.5	6.978
Z-22[a]	386	39.9	42	7.827

[a]Experiment conducted at .28 MPa (50 psi).

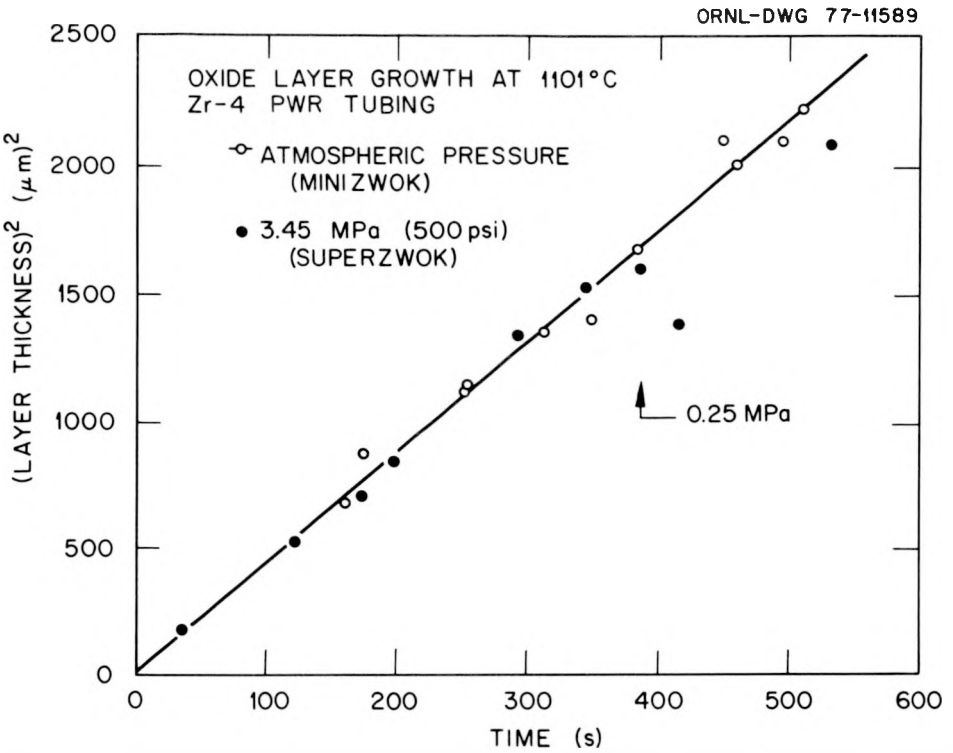

Fig. 1. Oxide Layer Growth During Oxidation of Sandvik Zircaloy-4 PWR Tubing at 1101°C (2014°F) in Steam at 3.45 MPa (500 psi) and at Atmospheric Pressure. Solid line represents MiniZWOK data.

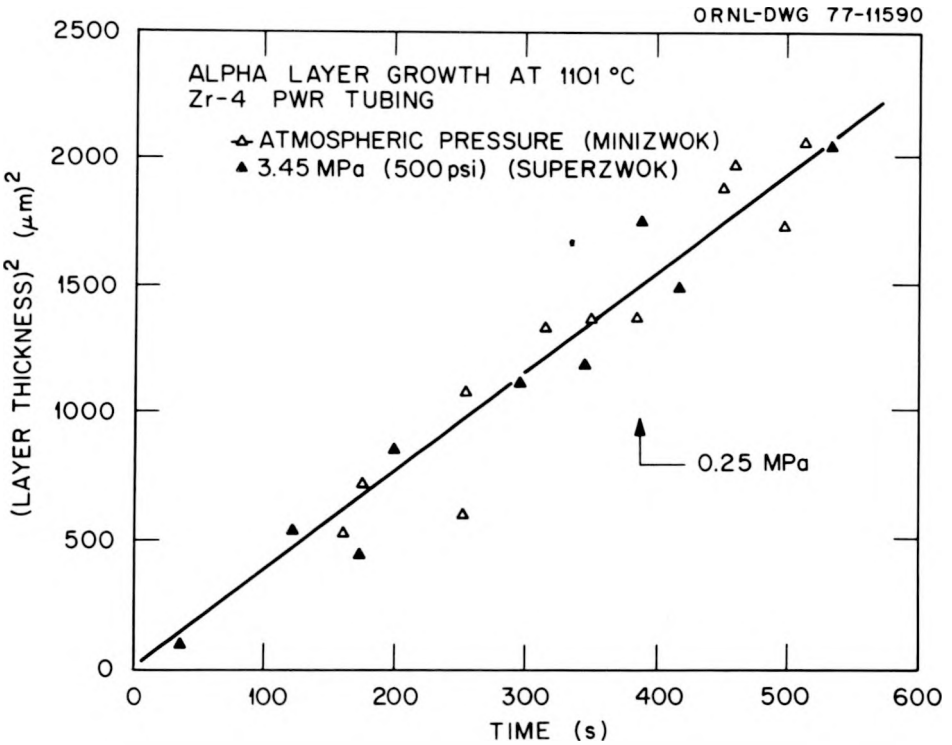

Fig. 2. Alpha Layer Growth During Oxidation of Sandvik Zircaloy-4 PWR Tubing at 1101°C (2014°F) in Steam at 3.45 MPa (500 psi) and at Atmospheric Pressure. Solid line represents MiniZWOK data.

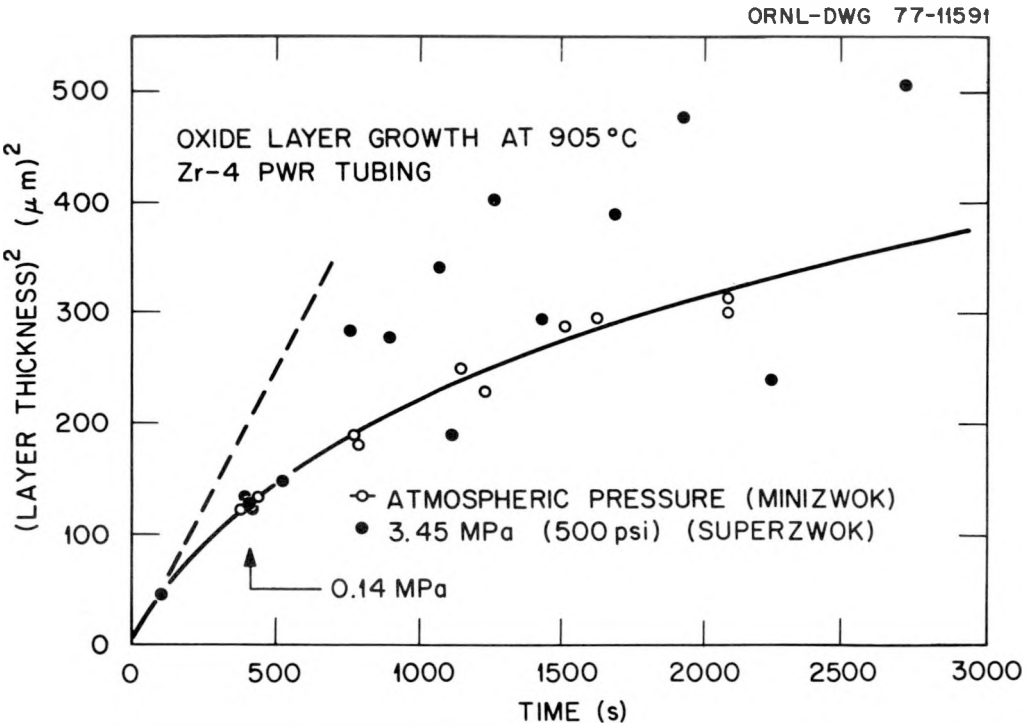

Fig. 3. Oxide Layer Growth During Oxidation of Sandvik Zircaloy-4 PWR Tubing at 905°C (1661°F) in Steam at 3.45 MPa (500 psi) and at Atmospheric Pressure. Dashed line represents kinetics extrapolated from high-temperature MiniZWOK data.

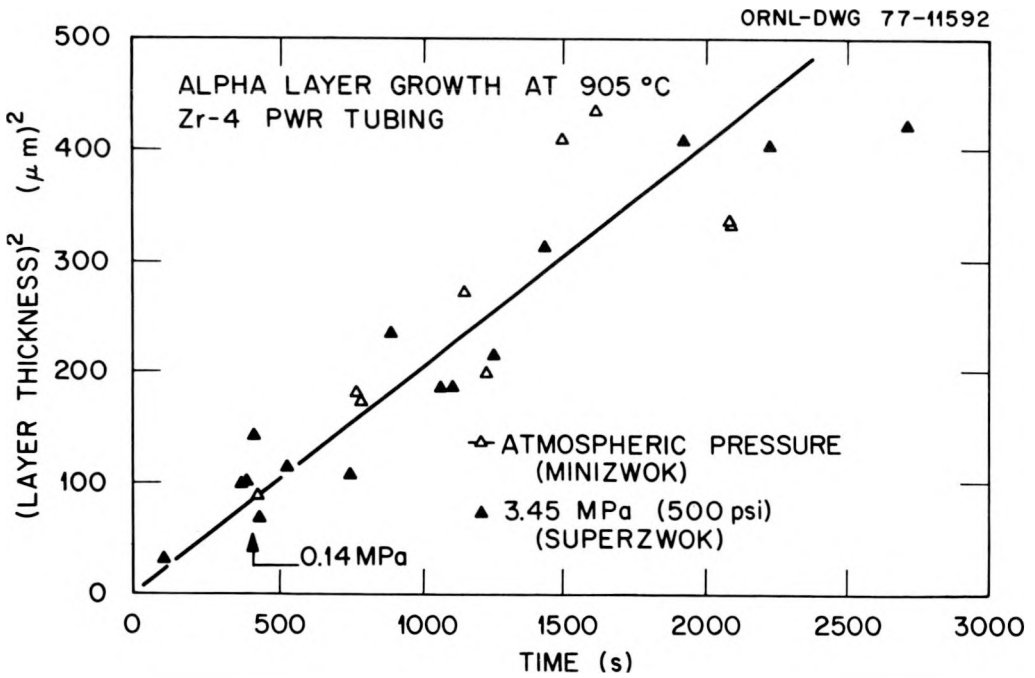

Fig. 4. Alpha Layer Growth During Oxidation of Sandvik Zircaloy-4 PWR Tubing at 905°C (1661°F) in Steam at 3.45 MPa (500 psi) and at Atmospheric Pressure. Solid line represents MiniZWOK data.

example of this characteristic is shown in Fig. 5, which shows a cross-section of a specimen oxidized in steam at 3.45 MPa (500 psi) at 905°C (1652°F) for 1069 s. While casual examination of the bright-field image does not indicate a layered oxide, in polarized light (and also dark-field) the duplex nature of the scale is revealed. To date, this behavior has been observed only in the long-time experiments in 3.45 MPa steam at 905°C (1661°F); the high-pressure experiments at 1101°C (2012°F), which for longer times produced oxide layers about twice as thick as those observed at 905°C (1661°F), did not exhibit this feature.

Although the occurrence of this "bright" oxide layer can be correlated with the formation of thicker than expected oxide layers on the 905°C (1652°F) SuperZWOK specimens, the reasons for its presence and the mechanism, if any, by which it could exert a kinetic influence are still matters for speculation. Since the oxidation temperature is in the range where pressure might be expected to influence the monoclinic-tetragonal transformation in the oxide,[4] it is possible that the kinetic influence is due to an increased proportion of the tetragonal phase in the oxide layer. It is observed, for example, that the rate of oxide layer growth, see Fig. 3, is less than that predicted from an extrapolation of the high-temperature data (dashed line), which corresponds to the formation of completely tetragonal oxide. On the other hand, 3.45 MPa seems to be a rather low pressure to exert such an effect.

It is also possible that we are dealing with a "breakaway" oxidation process in which a growing protective oxide layer suddenly becomes less protective because of cracking or other property changes. While the observed lack of reproducibility is characteristic of many such processes, we have no other evidence that this mechanism is responsible for the observed results.

Generally, data from the recent experiments are consistent with and reinforce the behavior suggested by previously reported results. At the 3.45 MPa level, no measurable effect was observed on the oxidation kinetics at 1101°C; at 905°C, the possibility of a small kinetic effect exists. We intend to perform several additional tests at 6.9 MPa (1000 psi), which should be useful in the further interpretation of the data.

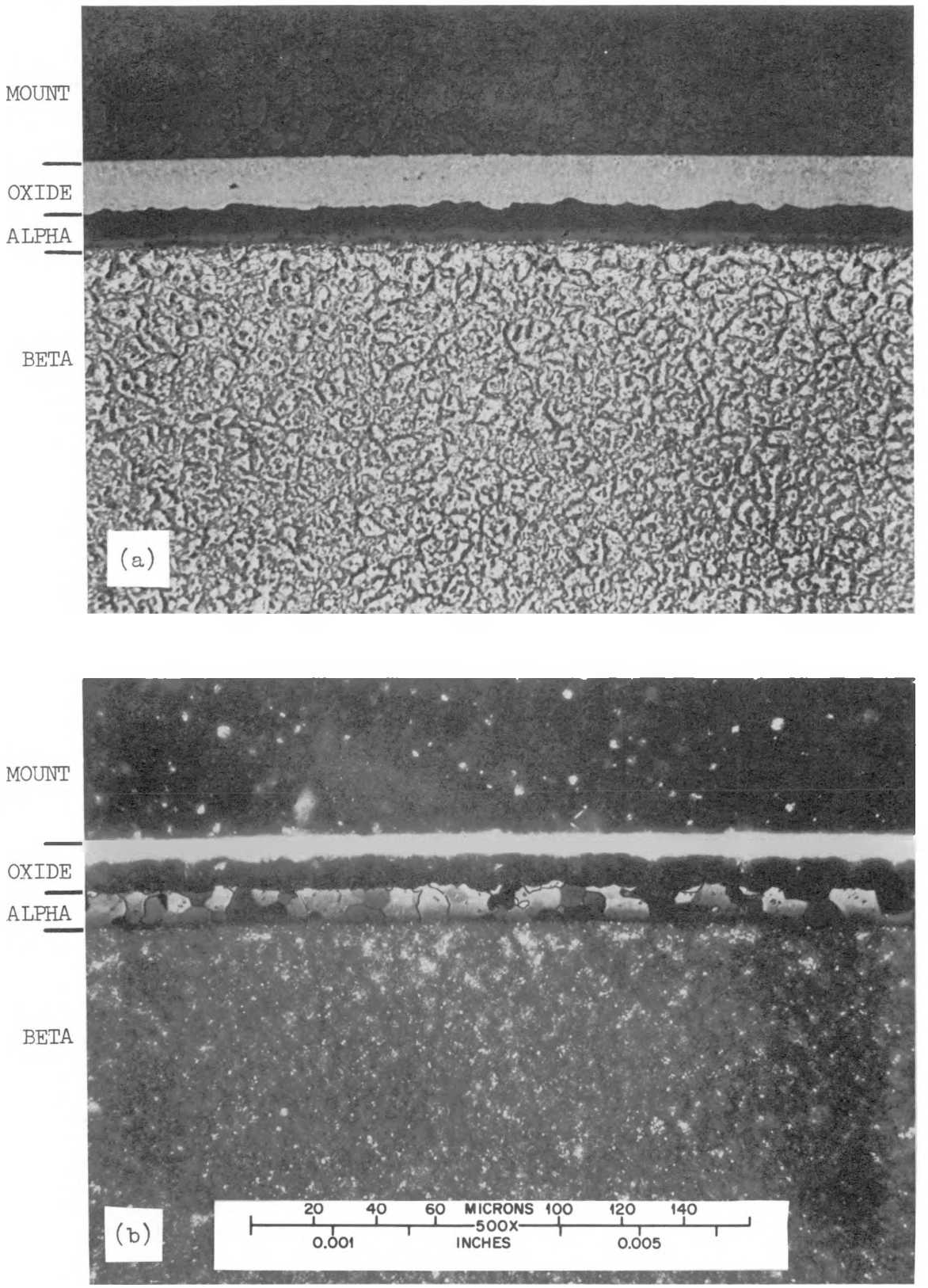

Fig. 5. Cross Section of Sandvik Zircaloy-4 PWR Tube Oxidized for 1069 s at 905°C (1661°F) in Steam at 3.45 MPa (500 psi) in SuperZWOK Apparatus. Expt. No. Z-44. 500×. (a) Bright-field illumination; (b) polarized light.

POSSIBLE EFFECTS OF DISSOLVED HYDROGEN ON THE OXIDATION RATES OF ZIRCALOY-4

R. A. McKee, R. E. Pawel, R. E. Druschel, and J. J. Campbell

In the previous Quarterly Report[1] we reported finding relatively large quantities of hydrogen in many oxidized MiniZWOK specimens. We showed that hydrogen concentration tended to increase with oxidation time, and we cited reasons for believing that the hydrogen entered the specimens through the interior of the specimens. During the past quarter we addressed the question of whether hydrogen dissolved in the metal phases of the specimens might have influenced the measured rates of oxidation.

There is a considerable body of indirect evidence that suggests that no such perturbation of the oxidation rates occurred, but as an additional check we also carried out a special series of oxidation experiments in which the MiniZWOK specimens were oxidized in pure oxygen rather than steam. In this section we describe these various observations and results and conclude finally that the presence of hydrogen in the metal did not, within the sensitivity of our measurements, influence oxidation rates.

Indirect Evidence

Self-Consistency of Rate Data

As reported previously,[1] the hydrogen content of the MiniZWOK specimens tended to increase with the total time of oxidation essentially independent of temperature or total oxygen consumption. Thus when a series of specimens was oxidized for varying lengths of time at a fixed temperature in order to generate an oxidation rate curve, the specimens oxidized for shorter times contained, in general, less hydrogen than those oxidized for longer periods [cf., MiniZWOK specimens oxidized at 1153°C (2107°F), Table 1, Ref. 1]. Yet no significant deviation from parabolic behavior was observed in the corresponding rate curves as might have been expected had hydrogen dissolved in the metal had a major effect on the kinetics.

A similar argument may be made regarding oxidation at different temperatures. Specimens oxidized at 1404°C (2559°F), for example, contained less hydrogen than those oxidized at 1153 (2107°F) because oxidation times at the higher temperatures were shorter. However, inspection of the Arrhenius plots of the rate data shows that the high temperature results are entirely consistent with those obtained at lower temperatures, again suggesting that the hydrogen dissolved in the metallic phases of the Zircaloy had no effect on oxidation rates.

We conclude, therefore, that the self-consistency of the oxidation rate data is itself evidence against spurious oxidation results relating to the absorption of hydrogen by the MiniZWOK specimens.

Comparison with Other Data

Oxidation rate data obtained with the MiniZWOK apparatus (relatively high hydrogen contents) agrees well with data obtained in the MaxiZWOK apparatus (low hydrogen) at 900 and 1000°C (1652–1832°F) and in the high pressure apparatus (SuperZWOK) where the hydrogen content of the specimens was also low (cf., Table 1). Similar good agreement can be cited between our data and those of Kawasaki, et al.[5] and Liestikow, et al.,[6] both the latter investigations involving specimens with low hydrogen contents. Thus a comparison of our MiniZWOK results with other data sets also supports the conclusion that hydrogen dissolved in Zircaloy has no appreciable effect on its oxidation rate.

Experiments in Pure Oxygen

Although the indirect evidence just cited suggests strongly that the hydrogen found in the MiniZWOK specimens did not influence their oxidation rate, we felt that the possibility of "hydrogen effects" actually occurring should not be dismissed out of hand. For example, the formation of O-H complexes, which could alter the diffusion rates of oxygen, has been observed near room temperature and below in niobium containing hydrogen and oxygen.[7,8] These complexes tend to dissociate at temperatures slightly above room temperature, making remote the likelihood of their existence in Zircaloy at temperatures of interest in this

study. Nevertheless, we have performed experiments in pure oxygen in order to provide a reference state against which possible hydrogen effects in Zircaloy can be judged.

Analysis of Possible Effects

At high temperatures ZrO_2 is generally assumed to be an n-type conductor with diffusion proceeding via an anion vacancy mechanism. Thus if hydrogen dissolved in the metal phases of a specimen has no effect on the oxidation rate and if no changes in stoichiometry, defect concentration, or ionic mobilities occur in the oxide, oxidation in pure oxygen should be identical with that observed for steam oxidation in the MiniZWOK apparatus. On the other hand, changes in mobility or equilibrium oxygen solubilities in oxide, alpha, or beta phases should cause oxidation behavior in pure oxygen to be different from that in steam, and it is possible to predict trends in the growth rates of oxide and oxygen-stabilized alpha layers on the basis of any such differences.

The velocity of any phase boundary in an oxidizing Zircaloy specimen is proportional to the difference between the oxygen fluxes into and out of the boundary. For example, the velocity, $\nu_{i,j}$ of the i,j boundary is given by

$$\nu_{i,j} = (J_{i,j} - J_{j,i})/\Delta c_{i,j} \tag{1}$$

and

$$J_{i,j} = -D_i \nabla c_{i,j} \tag{2}$$

where $J_{i,j}$ is the oxygen flux to the i,j boundary, the first subscript indicating the phase in which the flux is measured; $\nabla c_{i,j}$ is the oxygen concentration gradient in the i'th phase at the i,j boundary; D_i is the diffusion coefficient in the i'th phase; and $\Delta c_{i,j} = c_i - c_j$; with c_i and c_j being the equilibrium oxygen concentrations in the i'th and j'th phases, respectively, at the i,j boundary. Thus any change in $\nu_{i,j}$ must involve changes in diffusion coefficients or equilibrium oxygen concentrations or both. (Strictly speaking, the denominator of Eq. (1) should be written as $V_{i,j}\ C_{i,j} - C_{j,i}$, where $V_{i,j}$ is the ratio of equivalent

volumes of the i'th to the j'th phase. At the oxide-alpha boundary V has a value of 1.5 and is essentially unity at the α/β interface. In the discussion to follow the actual value of $V_{i,j}$ does not enter into consideration, and for the sake of notational simplicity we shall use Eq. (1) in the form shown with the understanding that $\Delta C_{i,j} \equiv V_{i,j} C_{i,j} - C_{j,i}$.)

Effects in the Alpha and Beta Phases. — It would appear that the only possible effect of hydrogen on D_α or D_β would be that of decreasing the diffusivities. As mentioned previously, changes in the diffusion coefficient for oxygen in Nb containing dissolved hydrogen could be brought about by the formation of the O-H complexes observed at low temperatures. It is most unlikely, however, that such complexes could retain any degree of stability in Zircaloy at the high temperatures used in this study, but if they do, the presence of the complexes should, if anything, reduce oxygen mobility. Both oxygen and hydrogen diffuse interstitially in Zircaloy, and the jump frequency, γ_{O-H}, for an O-H pair is related to the jump frequencies, Ω_O and Ω_H, of isolated oxygen and hydrogen atoms, respectively, by

$$\gamma_{O-H} = \Omega_O\Omega_H/(\Omega_O + \Omega_H) = \Omega_O/(1 + \Omega_O/\Omega_H) \quad , \tag{3}$$

and $\Omega_H > \Omega_O$. Therefore,

$$\gamma_{O-H} \leq \Omega_O \quad . \tag{4}$$

Thus the formation of O-H pairs should either reduce the diffusivity of oxygen or leave it unchanged. D_α or D_β might also be decreased if, as a result of the presence of hydrogen, the correlation factor for oxygen were reduced below the value of unity expected for interstitial diffusion. An increase in the diffusivity, on the other hand, would require that the strain field associated with dissolved hydrogen produce an increase in the jump frequency, Ω_O, for oxygen. In light of the smallness of the hydrogen atoms and their high rate of diffusion, however, such a possibility is dismissed, and we conclude that only decreases in D_α and D_β can occur as a result of the presence of hydrogen.

C. Roy[9] reports that when a crystal-bar zirconium sample, previously charged with 44 ppm tritium, was oxidized in oxygen at 500°C (932°F) long enough to produce an oxide film 2.5 μm thick, subsequent autoradiographs revealed no tritium in the oxide or in the underlying metal zone highly enriched in oxygen. When the oxidized specimens were annealed at 800°C (1472°F) to dissolve the oxide scale and then either slow cooled or quenched, "very little hydrogen was found in the thick layer of metal enriched in oxygen". Clearly, the introduction of oxygen into a Zircaloy specimen will reduce the solubility of hydrogen in the metal, and this result suggests the existence of a solubility product relationship

$$[a_O][a_H] = k \quad , \tag{5}$$

where a_O and a_H are the activities of oxygen and hydrogen, respectively, and k is the solubility product. Roy's experimental results indicate that the magnitude of any hydrogen effect in the alpha will surely be small, and the solubility product relationship suggests that hydrogen in the beta phase could only reduce the equilibrium oxygen solubility. Since a reduction of the solubility of oxygen in the beta would also lead to a reduction in $\nabla c_{\beta,\alpha}$, we can conclude that solubility changes due to hydrogen in the beta will produce only decreases in the oxygen flux, $J_{\beta,\alpha}$, into the beta [cf., Eq. (2)].

Effects in the Oxide — Kofstad's[10] summary of the properties of ZrO_2 makes it clear that transport mechanisms in ZrO_2 are not fully understood. The predominant characteristics of ZrO_2 are those of an oxygen-deficit, n-type semiconductor with material transport occurring via anion diffusion. Given the great stability of zirconia, the assumption of most investigators that ZrO_2 is stoichiometric in either steam or oxygen at one atmosphere might appear justified. With regard to the possible effects of the hydrogen liberated by the steam-Zircaloy reaction, we have already cited evidence for the limited solubility of hydrogen in ZrO_2,[9] and any effect of such small quantities of hydrogen on the vacancy diffusion rate in the oxide should be insignificant. On the basis of such arguments one would predict that oxygen mobilities and interfacial concentrations in the oxide would be the same during oxidation in oxygen or in steam.

On the other hand, electrical conductivity measurements at 1550°C (2822°F) and below provide somewhat controversial evidence for a component of p-character in the conductivity of ZrO_2. In such a case, the rate of oxidation might be some function of oxygen pressure. Furthermore, McClaine and Coppel[11] reported differences in the conductivity of ZrO_2 measured in H_2-H_2O atmospheres as compared to data obtained in CO-CO_2 mixtures having the same oxygen partial pressure. They attributed their results to hydrogen entering the ZrO_2 as an interstitial positive ion with an associated electron. These observations raise the possibility that during oxidation of Zircaloy in steam, small quantities of hydrogen dissolve in the oxide and change its defect concentration. For example, either an interstitial proton or a proton trapped on a vacant cation site would produce an increase in the oxygen vacancy concentration in the oxide. The influence of such hydrogen impurity atoms would be most important at the gas-oxide interface where the intrinsic vacancy concentration is virtually zero; at the oxide-alpha interface, however, the intrinsic vacancy concentration is so high (∿8%) as to make extrinsic contributions negligible. The net effect, then, of hydrogen dissolved in the oxide would be that of reducing slightly the defect concentration gradient across the scale by reducing the oxygen concentration in the oxide at the oxide-gas interface. For additional discussion of the role of hydrogen in the steam oxidation of Zircaloy, see Cox[12] and Hauffe and Martinez.[13]

The above comments relate to the properties of relatively pure ZrO_2. The oxide formed on Zircaloy contains small amounts of various alloying additions such as Sn, Fe, and Cr. Depending on their oxidation state, these impurity elements could contribute to the extrinsic defect concentration in Zircaloy oxide. However, in principle, at least, the various arguments given above should apply to both pure ZrO_2 and the oxide formed on the alloy.

We conclude from this discussion that it is difficult to suggest a mechanism by which oxygen mobility in the oxide can be affected by the oxidizing medium. However, the possibility of a variation in equilibrium solubilities cannot be dismissed. If such a change does occur, one should recognize that it is a natural consequence of oxidizing Zircaloy

in two widely differing media, and the change should not be described as a "hydrogen effect" in the sense of possible effects on oxidation rates produced by hydrogen dissolved in the alpha or beta regions.

Experimental Results for Oxidation in Oxygen

With these various possibilities in mind, oxidation rate curves were determined for Zircaloy-4 in 5—9's oxygen at 1253 and 1404°C (2287—2559°F). Ten specimens were used to define each curve, and the specimens and procedures used were identical to those employed in the standard MiniZWOK experiments except that pure oxygen at one atmosphere pressure was substituted for steam.

The results obtained are summarized in Table 3 in terms of parabolic rate constants for oxide and α-layer growth. The uncertainties listed define for the 90% confidence interval. For ease of comparison the corresponding rate constants obtained for oxidation in steam are also listed. Values of oxidation times, observed oxide and alpha layer thicknesses, and total oxygen consumed are tabulated in Tables 4 and 5.

Discussion of Results

Inspection of Table 3 shows that the rate of oxide growth is smaller in steam than in oxygen, while the rate of alpha growth is slightly greater in steam than in oxygen. At both temperatures investigated the differences in the two data sets are small, but the 90% confidence intervals for $\delta_\phi^2/2$ and $\delta_\tau^2/2$ do not overlap. The uncertainty intervals of $\delta_\alpha^2/2$ and $\delta_\xi^2/2$ do overlap at the 90% level; however, for both these parameters the trends in the experimental data are clear; the growth rate of the alpha layer is slightly greater in steam than in oxygen, while the reverse is true for Xi layer growth. We conclude, therefore, that the oxidation behavior of Zircaloy-4 in oxygen is not equivalent to oxidation in steam, and that

$$\phi\big|_{H_2O\text{-}\underline{H}} < \phi\big|_{O_2} \tag{6}$$

$$\alpha\big|_{H_2O\text{-}\underline{H}} > \alpha\big|_{O_2} \quad , \tag{7}$$

where ϕ and α are the oxide and alpha layer thicknesses, respectively. One may also infer from Eq. (6) that

Table 3. Parabolic Rate Constants for the Oxidation of Zircaloy-4 in Oxygen and Steam at 1253 and 1404°C (2287–2559°F)

Temperature [°C (°F)]	$\delta_\phi^2/2$ ($cm^2/s \times 10^7$)	Dev.[a] (%)	$\delta_\alpha^2/2$ ($cm^2/s \times 10^7$)	Dev.[a] (%)	$\delta_\xi^2/2$ ($cm^2/s \times 10^7$)	Dev.[a] (%)	$\delta_\tau^2/2$ [$(g/cm^2)^2/s \times 10^7$]	Dev.[a] (%)
				Oxidation in Oxygen				
1253 (2287)	0.9275	±3.1	0.9875	±4.9	3.827	±2.0	3.584	±1.9
1404 (2559)	2.681	±2.6	3.830	±5.2	12.92	±3.1	11.55	±2.1
				Oxidation in Steam[b]				
1253 (2287)	0.7663	±6.7	1.007	±8.2	3.530	±7.2	3.300	±6.0
1404 (2559)	2.351	±4.1	4.122	±4.4	12.70	±3.9	11.31	±3.4

[a]Uncertainty (%) at the 90% confidence level.

[b]Kinetic parameters in steam calculated from actual data at each temperature.

Table 4. Oxidation of Sandvik Zircaloy-4 PWR Tubing in Pure Oxygen at 1253°C (2287°)

Expt. No.	Time (s)	Oxide Layer (μm)	Alpha Layer (μm)	Total Oxygen (mg/cm^2)
S-225-TC-2	31.5	25.1	23.8	4.854
S-225-TC-3	34.1	25.6	24.7	4.972
S-256-TC-2	259.5	68.9	75.1	13.676
S-256-TC-3	254.5	67.1	73.4	13.351
S-257-TC-2	273.1	69.4	74.2	13.76
S-257-TC-3	266	70.1	71.3	13.755
S-258-TC-2	168.6	57.5	54.6	11.131
S-258-TC-3	158.7	55.7	53.5	10.802
S-259-TC-2	162.6	55.4	55.7	10.839
S-259-TC-3	152.9	54.3	54.4	10.606
S-260-TC-2	100.6	45	44.7	8.758
S-260-TC-3	103	45.4	44.1	8.809
S-261-TC-2	8.6	15.5	14.4	2.94
S-261-TC-3	9.5	15.8	14	2.985
S-262-TC-2	110.3	46.1	45.7	8.99
S-262-TC-3	102.8	44.9	44.7	8.753
S-263-TC-2	99.4	43.5	41.8	8.448
S-263-TC-3	100.2	43.2	40.4	8.366
S-264-TC-2	23.5	23.2	20.2	4.401
S-264-TC-3	23	23.1	21.6	4.424

Table 5. Oxidation of Sandvik Zircaloy-4 PWR Tubing in Pure Oxygen at 1404°C (2559°F)

Expt. No.	Time (s)	Oxide Layer (μm)	Alpha Layer (μm)	Total Oxygen (mg/cm^2)
S-265-TC-2	53	53.8	62	11.085
S-265-TC-3	52.2	53.3	61.3	10.979
S-266-TC-2	59.6	56.3	69.5	11.763
S-266-TC-3	60.5	57	66.4	11.777
S-267-TC-2	52.5	52.4	62.3	10.885
S-267-TC-3	53	53.3	62.6	11.03
S-268-TC-2	57.6	54.9	65.6	11.415
S-268-TC-3	57.9	55.4	68.8	11.59
S-269-TC-2	41.6	47	58.4	9.832
S-269-TC-3	41.5	46.8	57.7	9.78
S-270-TC-2	11.7	26.8	31.8	5.511
S-270-TC-3	12	27	30.5	5.495
S-271-TC-2	11.9	27.6	31.5	5.623
S-271-TC-3	12.7	28.1	33.6	5.783
S-272-TC-2	23.6	35.4	43	7.375
S-272-TC-3	23.8	36.4	43.4	7.535
S-273-TC-2	27.3	38.5	48.8	8.073
S-273-TC-3	27.6	38.4	45.8	7.97
S-274-TC-2	41.7	47.9	56.4	9.901
S-274-TC-3	38.9	45.6	53.8	9.446

$$\nu_{\phi,\alpha}|_{H_2O\text{-}\underline{H}} < \nu_{\phi,\alpha}|_{O_2} \quad . \tag{8}$$

Hydrogen Effects in the Beta Phase Only — The most immediate explanation that suggests itself for these differences is the possibility of a hydrogen effect in the beta phase. As already pointed out, most of the hydrogen in the MiniZWOK specimens must have been concentrated in the beta phase, and reasonable arguments can be made that other effects in the oxide and alpha layers should be minor. Consider, therefore, the following postulate, which we shall prove false.

Postulate I. A hydrogen effect occurs in the beta phase only. It follows from the postulate that mobilities and equilibrium oxygen concentrations are undisturbed in the oxide and alpha layers.

We shall now examine the experimental results for oxidation in steam and oxygen. The pertinent data are represented schematically in Fig. 6 where the positions of the various phase boundaries are referenced to the original metal surface. We consider the relative velocities of the oxide-alpha (ϕ-α) interfaces in steam and oxygen.

$$\nu_{\phi,\alpha} = (J_{\phi,\alpha} - J_{\alpha,\phi})/\Delta c_{\phi,\alpha} \quad . \tag{9}$$

Therefore,

$$\nu_{\phi,\alpha}|_{H_2O,\underline{H}} - \nu_{\phi,\alpha}|_{O_2} = \frac{1}{\Delta c_{\phi,\alpha}} [\underbrace{(J_{\phi,\alpha}|_{H_2O,\underline{H}} - J_{\phi,\alpha}|_{O_2})}_{\text{Term 1}}$$

$$\underbrace{- (J_{\alpha,\phi}|_{H_2O,\underline{H}} - J_{\alpha,\phi}|_{O_2})}_{\text{Term 2}}] \quad . \tag{10}$$

It can be seen from Fig. 6 that $\nabla c_{\phi,\alpha}|_{H_2O,\underline{H}} > \nabla c_{\phi,\alpha}|_{O_2}$ and $\nabla c_{\alpha,\phi}|_{H_2O,\underline{H}} < \nabla c_{\alpha,\phi}|_{O_2}$, and recalling that $J_{i,j} = D_i \nabla c_{i,j}$,

$$J_{\phi,\alpha}|_{H_2O,\underline{H}} > J_{\phi,\alpha}|_{O_2} \tag{11}$$

and

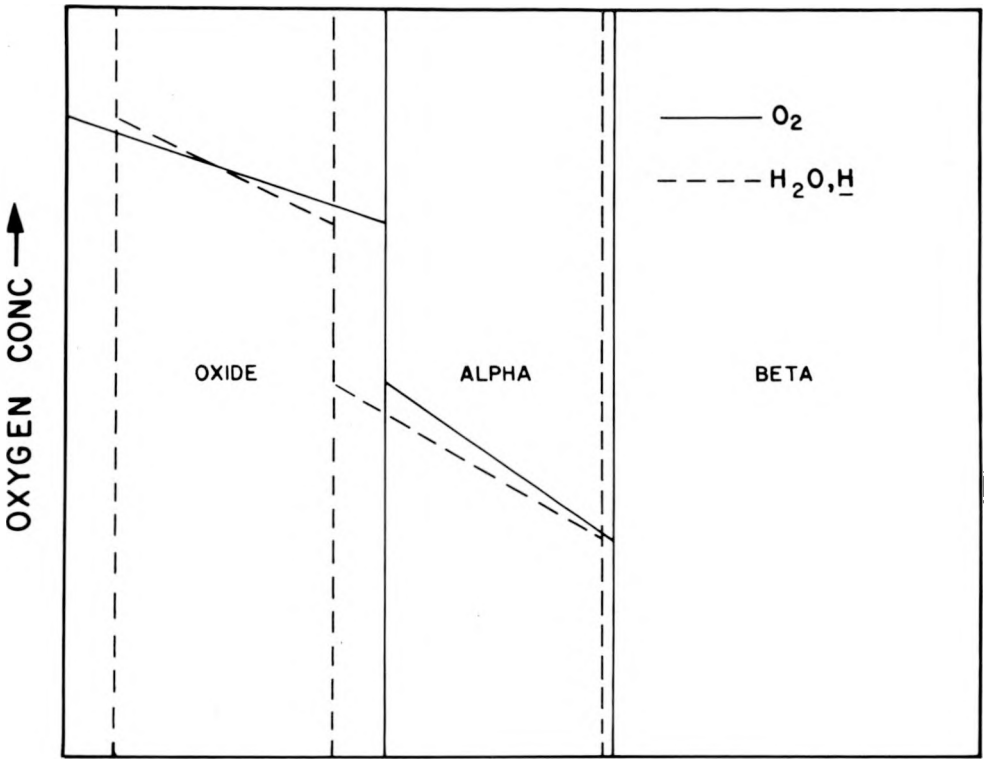

Fig. 6. Schematic Representation of Oxygen Concentration Gradients in Oxide and Oxygen-Stabilized Alpha Layers. The linear gradient shown in the oxide is a very good approximation of reality; the gradient in the alpha layer is certainly curved but is shown as linear in order to emphasize the differences in slope in steam as compared to oxygen. The arguments presented in the text turn on the relative values of ∇c at the various interfaces, and the relative differences in the values are the same whether the actual gradient across the phase is linear or a function of position.

$$J_{\alpha,\phi}\big|_{H_2O,\underline{H}} < J_{\alpha,\phi}\big|_{O_2} \quad ? \tag{12}$$

Referring Eqs. (11) and (12) to Eq. (10), it is evident that Postulate I requires the right side of Eq. (10) to be a positive quantity, while the experimental observation [cf., Eq. (8)] shows that the left side of the equation is negative. Therefore, Postulate I is false; the differences between oxidation in steam and in oxygen cannot be explained in terms of a hydrogen effect in the beta alone.

Effects in the Oxide Only — We consider now a second postulate concerning the possibility that the decrease in oxide growth rate and the increase in the alpha growth rate in steam relative to oxygen is due to

a decreased oxygen flux into the oxide for oxidation in steam. We shall show that this idea is consistent with the experimental results.

Postulate II. The oxygen flux into the oxide is smaller in steam than in oxygen, and oxygen mobilities in the α and β phase remain unchanged as do the equilibrium oxygen concentrations at the ϕ,α and α,β boundaries.

This postulate is consistent with the experimental observations as may be seen from the following arguments. By Postulate II

$$J_{\phi,\alpha}\big|_{H_2O,\underline{H}} < J_{\phi,\alpha}\big|_{O_2} \quad ; \tag{13}$$

therefore, the first term on the right side of Eq. (10) is negative. Referring again to the oxygen concentration gradients in the alpha phase (Fig. 6), it is evident that Eq. (12) holds in this case also; therefore, the second term on the right of Eq. (10) is negative and makes a net positive contribution in light of the negative sign in front of it. The left side of the equation is negative, requiring only that

$$|\text{Term 1}| > |\text{Term 2}|$$

in order to satisfy the experimental observations.

This type of analysis can also be extended to take into account the relative velocities of the α/β interface.

$$\nu_{\alpha,\beta}\big|_{H_2O,\underline{H}} - \nu_{\alpha,\beta}\big|_{O_2} = \frac{1}{\Delta c_{\alpha,\beta}} [\underbrace{(J_{\alpha,\beta}\big|_{H_2O,\underline{H}} - J_{\alpha,\beta}\big|_{O_2})}_{\text{Term 1}}$$

$$\underbrace{- (J_{\beta,\alpha}\big|_{H_2O,\underline{H}} - J_{\beta,\alpha}\big|_{O_2})}_{\text{Term 2}}] \quad . \tag{14}$$

The experimental observation is that

$$\xi\big|_{H_2O,\underline{H}} < \xi\big|_{O_2} \quad , \tag{15}$$

where ξ is the combined oxide and alpha layer thickness, and when the position of the α/β interface was referenced to the original metal surface, we found

$$\nu_{\alpha,\beta}|_{H_2O,\underline{H}} \leq \nu_{\alpha,\beta}|_{O_2} \quad . \tag{16}$$

Therefore, the left side of Eq. (14) is equal to or slightly less than zero. As previously, Term 1 on the right side of Eq. (14) is negative. Since the position of the α,β boundary is almost the same in the two oxidizing media, it is likely that Term 2 in Eq. (14) is close to zero, but in any event, we only require that |Term 1| ≥ |Term 2|. Thus we conclude that Postulate II is consistent with the experimental results.

It is, in fact, possible to offer supplementary evidence that changes in oxide stoichiometry are responsible for the observed differences for oxidation in steam and in oxygen. This additional evidence involves the observation that a line of metallic particles, rich in tin, is found in cross sections through the oxide formed on Zircaloy tubes oxidized in either steam or oxygen. This phenomenon has been reported in detail previously,[14] and the key fact is that the oxide is divided into inner and outer regions by the particle line with the ratio of the inner oxide layer thickness, ϕ_i, to that of the outer layer, ϕ_o, being essentially constant with oxidation time. Since the oxygen concentration gradient across the oxide is virtually linear, the constancy of ϕ_o/ϕ_i indicates that the metallic particles must form and move along a plane of constant oxygen potential in the oxide.

Values of ϕ_o and ϕ_i were obtained for specimens oxidized in steam and in oxygen at 1253 and 1404°C (2287—2559°F), and the results are summarized in Table 6. In both oxidizing media the ratio of inner to outer oxide thickness, ϕ_i/ϕ_o, is constant with both time and total oxide thickness; however, the inner oxide is relatively thicker in steam than oxygen.

These results underscore some interesting aspects of the differences in the oxidation behavior of Zircaloy in steam and oxygen. Assuming only that the constant oxygen potential at which the metallic particles form is the same in both media, the fact that ϕ_i/ϕ_o is different in the two cases means that the equilibrium oxygen content of the oxide at one or both interfaces is different in steam than in oxygen. Furthermore, as will be demonstrated graphically below, the fact that $\phi_i/\phi_o|_{H_2O,\underline{H}} > \phi_i/\phi_o|_{O_2}$ indicates that the difference between the oxygen concentration

Table 6. Comparison of Growth Rates and Thickness Ratios of Inner and Outer Oxide Layers Formed in Steam and Oxygen

	Temperature [°C (°F)]	
	1253 (2287)	1404 (2559)
$\delta_\phi^2/2\|_{O_2} \times 10^8$ (outer oxide)	3.44 ± 10.6%	8.47 ± 11.8%
$\delta_\phi^2/2\|_{O_2} \times 10^8$ (inner oxide)	1.45 ± 5.9%	5.12 ± 4.9%
$\delta_\phi^2/2\|_{H_2O,\underline{H}} \times 10^8$ (outer oxide)	2.33 ± 9.7%	7.40 ± 6.9%
$\delta_\phi^2/2\|_{H_2O,\underline{H}} \times 10^8$ (inner oxide)	1.55 ± 7%	5.25 ± 3.2%
$\phi_i/\phi_o\|_{O_2}$	.649	.777
$\phi_i/\phi_T\|_{O_2}$	.394	.437
$\phi_i/\phi_o\|_{H_2O,\underline{H}}$	.815	.842
$\phi_i/\phi_T\|_{H_2O,\underline{H}}$	.449	.457

at the oxide-gas interface, $c_{\phi,g}$, and that, $c_{\phi,\alpha}$, at the oxide-alpha interface in steam is less than the corresponding difference, $c_{\phi,g}-c_{\phi\,\alpha}$, in oxygen. This condition is precisely one of the phenomena in the oxide previously suggested as a cause of the differences in the oxidation behavior of Zircaloy in oxygen and steam.

These experimental results can be used as a quantitative basis for assessing the extent and nature of the "hydrogen effect" in the oxide. Figure 7 is a schematic representation of the oxygen concentration gradient across a Zircaloy oxide scale. Note that the triangle $c_{\phi,g}$,A,$c_{\phi,\alpha}$ is similar to the triangle C,B,$C_{\phi,\alpha}$; therefore,

$$\frac{C - C_{\phi,\alpha}}{\phi_i} = \frac{C_{\phi,g} - C_{\phi,\alpha}}{\phi_T} \tag{17}$$

or

$$\frac{\phi_i}{\phi_T} = \frac{C - C_{\phi,\alpha}}{C_{\phi,g} - C_{\phi,\alpha}} \quad , \tag{18}$$

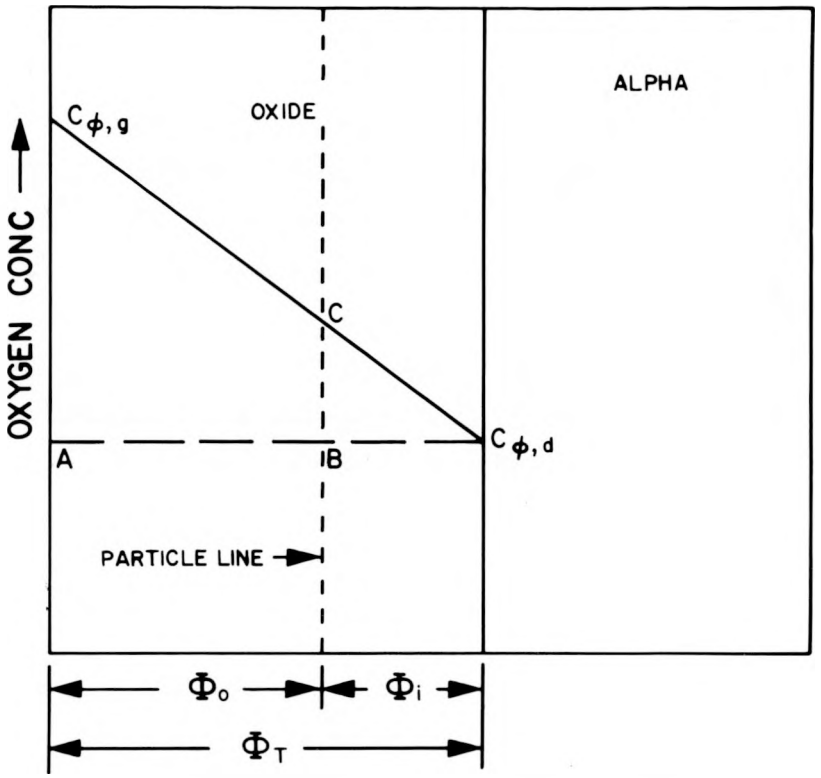

Fig. 7. Schematic Representation of Oxygen Concentration Gradient in the Oxide Layer Showing Position of the Tin-Rich Particle Line.

where $\phi_T = \phi_o + \phi_i$ is the total oxide thickness. Equation (18) is valid for oxidation in either steam or oxygen. Note also that Eq. (18) demonstrates that the ratio ϕ_i/ϕ_T is independent of any effect attributable to the presence of dissolved hydrogen in the oxygen-stabilized α or the β phases.

One may now form the ratio

$$\frac{(\phi_i/\phi_T)|_{H_2O,\underline{H}}}{(\phi_i/\phi_T)|_{O_2}} = \frac{\dfrac{C - C_{\phi,\alpha}}{C_{\phi,g}|_{H_2O,\underline{H}} - C_{\phi,\alpha}}}{\dfrac{C - C_{\phi,\alpha}}{C_{\phi,g}|_{O_2} - C_{\phi,\alpha}}} \tag{19}$$

or

$$\frac{(\phi_i/\phi_T)|_{H_2O,\underline{H}}}{(\phi_i/\phi_T)|_{O_2}} = \frac{C_{\phi,g}|_{O_2} - C_{\phi,\alpha}}{C_{\phi,g}|_{H_2O,\underline{H}} - C_{\phi,\alpha}} \quad . \tag{20}$$

On the basis of phase diagram information the equilibrium oxygen concentrations at the oxide-alpha boundary, $C_{\phi,\alpha}$, are 1.403 and 1.391 gm/cc at 1253 and 1404°C (2287–2559°F), respectively.[15] Taking the oxide at the oxide-gas interface to be stoichiometric in pure oxygen ($C_{\phi,g}|_{O_2}$ = 1.511 gm/cc), the appropriate experimental values of ϕ_i/ϕ_T (Table 6) may be used to calculate $C_{\phi,g}|_{H_2O,\underline{H}}$. The result at both temperatures is $C_{\phi,g}|_{H_2O,\underline{H}}$ = 1.50 gm/cc, which is equivalent to $ZrO_{1.99}$.

The "particle line" observations thus indicate that oxidation in steam produces a reduction in $\nabla C_{\phi,\alpha}$ as compared to oxidation in oxygen. However, the flux across the oxide-gas interface is the product of $\nabla C_{\phi,\alpha}$ and the chemical diffusion coefficient, D_ϕ, for the oxide

$$J_{\phi,g} = -D_\phi \nabla C_{\phi,\alpha} \quad . \tag{21}$$

We now demonstrate that the variation of $\nabla C_{\phi,\alpha}$ deduced from the particle line observations can alone account for the differences in oxidation in oxygen as compared to steam, in other words, that $D_\phi|_{O_2} = D_\phi|_{H_2O,\underline{H}}$.

An analytical expression for D_ϕ may be obtained from Eq. (21) by noting that

$$J_{\phi,g} = -D_\phi \nabla C_{\phi,\alpha} = D_\phi (C_{\phi,g} - C_{\phi,\alpha})/\phi = d\tau/dt \quad , \tag{22}$$

where τ is the total oxygen consumed by the sample. From the fundamental equations describing parabolic oxidation kinetics, we have

$$d\tau/dt = (\delta_\tau^2/2)/\tau \quad , \tag{23}$$

$$\tau = \delta_\tau \sqrt{t} \quad , \tag{24}$$

and

$$\phi = \delta_\phi \sqrt{t} \quad . \tag{25}$$

Using Eqs. (23) and (24),

$$d\tau/dt = \delta_\tau/2\sqrt{t} \quad , \tag{26}$$

and substituting Eq. (26) into Eq. (22), using Eq. (25), and solving for D_ϕ, we obtain

$$D_\phi = \delta_\tau \delta_\phi / 2(C_{\phi,g} - C_{\phi,\alpha}) \quad . \tag{27}$$

Equation (26) is valid for both oxidizing media; therefore, we may form the ratio

$$\frac{D_\phi|_{H_2O,\underline{H}}}{D_\phi|_{O_2}} = \frac{(\delta_\tau \delta_\phi)_{H_2O,\underline{H}}}{(\delta_\tau \delta_\phi)_{O_2}} \left[\frac{C_{\phi,g}|_{O_2} - C_{\phi,\alpha}}{C_{\phi,g}|_{H_2O,\underline{H}} - C_{\phi,\alpha}} \right] \quad . \tag{28}$$

If the diffusion coefficient in the oxide is the same for oxidation in steam as in oxygen, obviously, the ratio $D_\phi|_{H_2O,\underline{H}}/D_\phi|_{O_2}$ must be unity.

We evaluate Eq. (28) using the value of $C_{\phi,g}|_{H\ O,\underline{H}} = 1.50$ gm/cc obtained from the "particle line" observations; values for $C_{\phi,\alpha}$ are based on the phase diagram data already cited; $C_{\phi,g}|_{O_2} = 1.511$ gm/cc; and δ_τ and δ_ϕ values are derived from the oxidation data for oxidation in oxygen (see Table 3) and from values for $\delta_\tau^2/2$ and $\delta_\phi^2/2$ obtained from the standard MiniZWOK data set at 1253 and 1404°C (2287—2559°F). The results obtained were

$$D_\phi|_{H_2O,\underline{H}}/D_\phi|_{O_2} = 0.971 \text{ at } 1253°C \text{ } (2287°F) \tag{29}$$

and

$$D_\phi|_{H_2O,\underline{H}}/D_\phi|_{O_2} = 1.02 \text{ at } 1404°C \text{ } (2559°F) \quad . \tag{30}$$

These results show that the ratio of oxide diffusion coefficients is certainly unity within experimental uncertainty, and it is interesting to dwell on the implications of this conclusion. Unlike Eq. (20), where all quantities on the left side of the equation are direct observations and independent of hydrogen effects in either the α or β regions, the right side of Eq. (28) involves the product of δ_τ and δ_ϕ, both of which could be influenced by hydrogen effects in the α and β. Furthermore, while δ_ϕ is an experimental quantity based on observations of oxide thickness as a function of time, δ_τ is a calculated value in our study. Its evaluation requires not only direct measurements of oxide and alpha

layer thicknesses, but also information concerning oxygen diffusivity in the beta and oxygen interfacial equilibrium concentrations in the various phases. All the latter values were determined (by us or others) in the absence of hydrogen. Thus the numerical evaluation of the right side of Eq. (28) as we have performed it is "biased" in the sense that a significant hydrogen effect in the α or β phases, if it existed, would cause the real value of δ_τ to be different from that which we calculated with the result that the ratio of diffusivities would depart from unity. However, no such bias is evident in the results shown in Eqs. (29) and (30), and we are led to the following conclusions.

1. The value of $\nabla C_{\phi,g}$ for oxidation in oxygen is greater than that in steam because of a reduction in $C_{\phi,g}$ during oxidation in steam.

2. The differences in oxidation behavior in the two media may be rationalized solely in terms of a variation in $\nabla C_{\phi,g}$; D_ϕ remains unchanged.

3. Implicit in these results is the conclusion that hydrogen dissolved in the alpha and beta phases does not change the oxygen interfacial concentrations in either the α or β, nor does it influence oxygen diffusivity in the beta.

This last conclusion may be tested more directly through a calculation of the diffusivity, D_α, for oxygen in the alpha. Pawel[15] has shown that D_α may be expressed as

$$D_\alpha = \frac{1}{F}\left\{\left[\left(\frac{\delta_\alpha^2}{2} + \frac{\frac{1}{V}\,\delta_\phi\delta_\alpha}{2}\right)\left(\frac{C_{\alpha,\beta} - C_{\beta,\alpha}}{C_{\alpha,\phi} - C_{\alpha,\beta}}\right)\right] + \left[\frac{\delta_\alpha\sqrt{D}_\beta\,(C_{\beta,\alpha} - C_\beta)}{\sqrt{\pi}\,(C_{\alpha,\phi} - C_{\alpha,\beta})}\right]\frac{\left[\exp -\left(\frac{\delta_\alpha + \frac{1}{V}\,\delta_\phi}{2\sqrt{D_\beta}}\right)^2\right]}{\left[1 - \operatorname{erf}\left(\frac{\delta_\alpha + \frac{1}{V}\,\delta_\phi}{2\sqrt{D_\beta}}\right)\right]}\right\} \tag{31}$$

where

C_β is the initial oxygen concentration in the beta phase, and

$$F = \frac{\frac{\delta_\alpha}{\sqrt{\pi D_\alpha}} \exp - \left(\frac{\delta_\alpha + \frac{1}{V}\delta_\phi}{2\sqrt{D_\alpha}}\right)^2}{\operatorname{erf}\left(\frac{\delta_\alpha + \frac{1}{V}\delta_\phi}{2\sqrt{D_\alpha}}\right) - \operatorname{erf}\left(\frac{\frac{1}{V}\delta_\phi}{2\sqrt{D_\alpha}}\right)} .$$

Inspection of Eq. (31) shows that all the parameters on the right side, save only V, could, in principle, be changed by the existence of a hydrogen effect in the alpha or beta phases. Note also that the δ_i's are are quantities derived directly from our experimental data, while values for D_β and the equilibrium oxygen concentrations have been obtained only in the absence of significant amounts of dissolved hydrogen in the α and β phases. Thus the use of Eq. (31) to evaluate $D_\alpha|_{O_2}$ and $D_\alpha|_{H_2O,\underline{H}}$ is "biased" in the sense that the existence of any hydrogen effect that changes D_β or the oxygen concentration terms would cause the calculated value of D_α to be different from the real value. Consequently, if one finds, on the basis of Eq. (31), that $D_\alpha|_{O_2} \neq D_\alpha|_{H_2O,\underline{H}}$, a hydrogen effect in the alpha or beta is strongly suggested. On the contrary, the finding that $D_\alpha|_{O_2}$ equals $D_\alpha|_{H_2O,\underline{H}}$ provides compelling evidence that no significant hydrogen effect exists.

Substitution of appropriate values for the parameters in Eq. (31) yields the results shown in Table 7. Clearly, within experimental accuracy $D_\alpha|_{O_2} = D_\alpha|_{H_2O,\underline{H}}$, and we conclude as before that the presence of dissolved hydrogen in the α and β phases had no significant effect on the observed rates of oxidation of our standard MiniZWOK specimens.

Table 7. Comparison of D_α Calculated from Oxidation Rate Data Obtained in Steam and Oxygen

Temperature		$D_\alpha\|_{O_2}$	$D_\alpha\|_{H_2O}$ [a]	Diff. [b]
°C	(°F)	($cm^2/s \times 10^7$)	($cm^2/s \times 10^7$)	(%)
1253	(2287)	1.99	1.95	2.1
1404	(2559)	8.67	8.86	−2.1

[a] Values calculated from analytical expressions for diffusion coefficients derived from standard MiniZWOK data (see Ref. 15).

[b] Difference relative to oxidation in steam.

The arguments presented thus far demonstrate that the differences observed in oxidation behavior of Zircaloy in oxygen and in steam are consistent with differences in the oxygen flux into the oxide in the two media and are inconsistent with the existence of an appreciable hydrogen effect in the α or β phases. One final test of the experimental results can be cited in support of this conclusion. We again suggest an oxidation model (that will be shown to be incorrect) that is not inconsistent with the interface velocity equations [Eqs. (10) and (14)], and we require the following assumptions:

$$J_{\phi,\alpha}|_{H_2O,\underline{H}} < J_{\phi,\alpha}|_{O_2} \tag{32}$$

$$J_{\alpha,\beta}|_{H_2O,\underline{H}} < J_{\alpha,\beta}|_{O_2} \tag{33}$$

and

$$J_{\beta,\alpha}|_{H_2O,\underline{H}} < J_{\beta,\alpha}|_{O_2} \ . \tag{34}$$

This model cannot be correct, however, because, as we shall now demonstrate, the conditions contained in Eqs. (32)—(34) require a departure from parabolic growth kinetics for both oxide and alpha layer growth.

Consider the implications of Eq. (32)—(34). Not only is the flux into the oxide different in steam compared to oxygen [Eq. (32)], but the hydrogen dissolved in the alpha and beta regions is also assumed to reduce the oxygen flux into these phases. We suppose now that the Zircaloy is oxidized in steam under conditions where no hydrogen dissolves in the metallic phases of the specimen, and we contrast the resulting oxidation behavior to that exhibited when "hydrogen effects" are present in both the α and β. Since steam is the oxidizing medium in both cases, we expect no differences in interfacial equilibrium oxygen concentrations or mobilities in the oxide. By contrast, the postulate that hydrogen dissolved in the specimen reduces the flux of oxygen in the α and β phases means that the "hydrogen effect", by reducing $J_{\alpha,\phi}$, actually increases the velocity of the oxide-alpha interface relative to its velocity in steam in the absence of dissolved hydrogen; that is

$$\nu_{\phi,\alpha}|_{H_2O,\underline{H}} > \nu_{\phi,\alpha}|_{H_2O} \quad , \tag{35}$$

where the notation "$|_{H_2O}$" refers to steam oxidation in the absence of dissolved hydrogen. In other words, if Eqs. (32)—(34) are valid, the rate of oxide growth in steam in the absence of dissolved hydrogen is less than that in the case where hydrogen is present. The resulting oxidation rate curves are shown schematically in Fig. 8.

As already noted, hydrogen analyses of oxidized MiniZWOK specimens exhibited considerable variability, but there was a general tend for hydrogen content to increase with oxidation time. The analytical data are not good enough to establish a functional relationship between hydrogen content and time, but in no case is there any evidence that the specimens become saturated with hydrogen. Therefore, it follows from

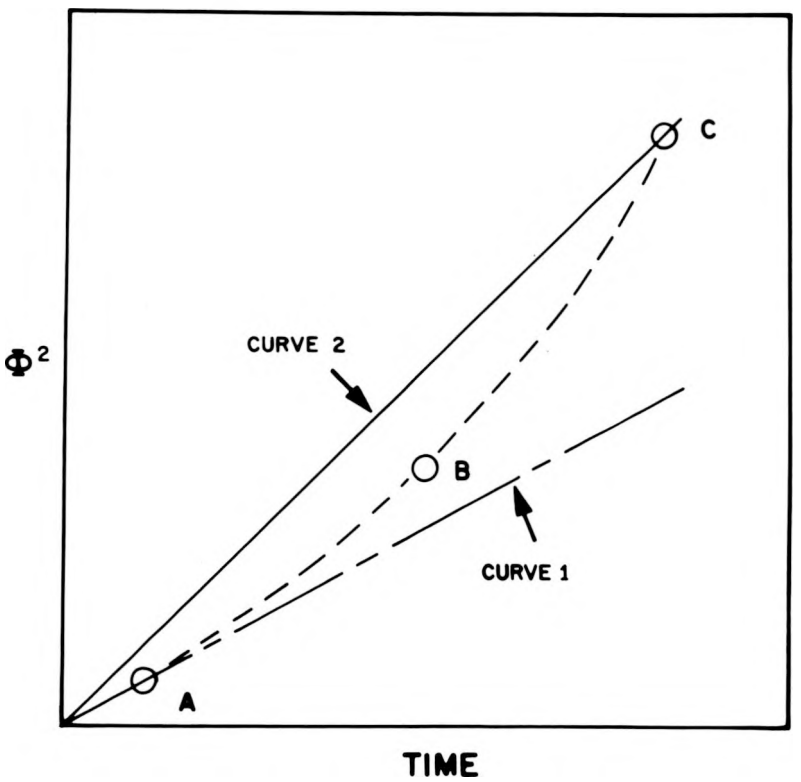

Fig. 8. Schematic Representation of Hypothetical Oxide Growth Rates for Zircaloy Without Dissolved Hydrogen (Curve 1) and with Dissolved Hydrogen (Curve 2). The dashed line shows the expected rate curve assuming a "hydrogen effect" and given the condition that the hydrogen content increases with time.

the model that the rate of oxidation of a specimen oxidized for a short time should be less influenced by hydrogen than is the case for a relatively long oxidation time. The resulting rate curve would then be expected to have the formed defined by the points A, B, and C in Fig. 8; short-time specimens should yield oxide thicknesses close to those predicted by Curve 1 (e.g., point A). On the other hand a long-time specimen should produce a datum such as point C near Curve 2. The net result would be an oxidation rate curve that is concave upward. Inspection of the oxidation rate curves show no such trend. We estimate that a "hydrogen effect" that led a maximum increase in oxide thicknesses of 10% for long time samples would produce a very obvious upward curvature in the rate curve and that a 5% effect should be detectable. Clearly, the postulated "hydrogen effects" either do not exist or are at worst small.

Another way of stating the above argument is to note that a "hydrogen effect" that increases with time perturbs the kinetics of oxidation, causing a departure from the Parabolic Rate Law. Thus the discussion above relative to the growth rate of the oxide is also applicable to the growth of the alpha layer. As in the case of the oxide, inspection of the alpha layer rate curves shows that they are well represented by a parabolic oxidation model and exhibit no indication of a hydrogen effect.

Conclusions

The dissolved hydrogen detected in MiniZWOK specimens was shown to be an artifact of the experimental procedure used. A variety of tests were performed to determine whether this dissolved hydrogen influenced the measured rates of oxidation. These tests included

1. The internal consistency of the data;
2. Comparisons with other data sets (our own and those of other investigators);
3. Oxidation rate measurements in pure oxygen.

In no case was any evidence of a "hydrogen effect" found, and we concluded that within the limits of experimental uncertainty our measured values of

oxide and alpha layer growth rates were unaffected by the presence of hydrogen in the metallic phases of the specimens.

EVALUATION OF THERMAL SHUNTING ERRORS IN MINIZWOK

R. A. McKee and R. E. Druschel

As a part of our general concern for and in consideration of the need of accurate temperature measurements in the ZWOK program, various experiments have been performed during the entire program effort to establish temperature measurement uncertainties. Particularly in the MiniZWOK apparatus, which has provided the base isothermal oxidation data set, the experimental checks have been exhaustive. Aside from external calibration of component parts in the thermometry assembly,[16] *in situ* tests have been performed to evaluate the thermometry capabilities under operating conditions. The two areas of operating conditions that cause particular concern in high temperature thermometry are electrical and thermal shunting errors, and in past quarterlies documentation has been provided for evaluation of potential electrical shunting errors, but a definitive experiment for evaluation of potential thermal shunting errors has not been reported. In the thermometry report[11] calculations were made which set liberal limits for an estimation of thermal shunting errors, but experimental confirmation has been difficult. In this past quarter the definitive experiment has been performed and establishes the quantitative thermal shunting error in the MiniZWOK apparatus.

To evaluate the thermal shunting error in a temperature measurement, the specimen must be held at a known temperature and that temperature compared to the apparent specimen temperature as recorded by the thermocouple. The experiment used to establish this comparison is not an easy one to perform because of obvious uncertainties in the true specimen temperature. After much trial and error, a unique experiment was performed in the MiniZWOK apparatus that fully satisfies the constraints placed on a successful evaluation of the thermal shunting error.

In the MiniZWOK apparatus the oxidizing tube is heated from the outside by a radiant heating furnace while the temperature is measured

with thermocouples placed on the inner surface, and in this arrangement there is a potential for thermal shunting. For a proper evaluation of the thermal shunting due to the thermocouple placement, the oxide temperature of the oxide-gas interface must be known. To accomplish this, melting-point-standard gold* was held in a cruicble formed from the concentric placing of a BWR tube over a PWR tube as indicated in Fig. 9. Before the gold was placed in the crucible, the thermocouples were mounted

*Marz Gold obtained from Materials Research Corp. Vendor certified analysis (ppm by wt): 15 C, <5.0 O, <1.00 H, <5.0 N, 0.20 Al, 0.10 Na, 0.02 Mg, <0.01 P, 0.13 S, 0.16 Cl, 0.40 K, 0.30 Ca, 0.01 Ti, 0.73 Fe, 1.30 Cu, 0.51 Si, <0.01 Cr, 0.05 Ni, 0.05 Zn, 0.06 Mo, 0.25 Pd, 4.20 Ag, <0.01 Sn, 0.02 Sb, <0,01 Pb.

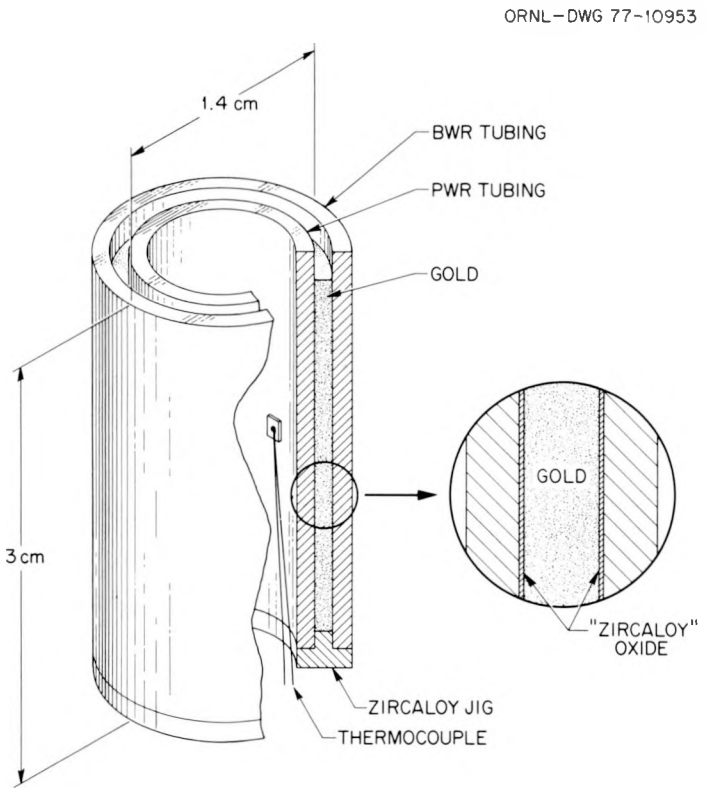

Fig. 9. Schematic Drawing of "Zircaloy Oxide" Crucible Used in Gold-Point Determination.

in the standard fashion for specimen instrumentation, and the outer BWR, inner BWR, and outer PWR surfaces were oxidized to form the oxide-α-beta phase relationship present in a standard experiment. The oxide thickness was approximately 30 μm. The specimen-crucible was then removed from the apparatus, the gold foil inserted, and the entire assemblage placed back into the apparatus for the measurement. The subsequent melting of the gold was done with flowing helium as an environment. The specimen was first driven through the melting point of gold to bring the gold into intimate contact with the oxide surface and then again driven through the transient pictured in Fig. 10. This mode of heating was identical to that in an oxidation experiment except that when the temperature reached the melting point of gold, a thermal arrest occurred, causing the oxide-gold interface to be at a fixed and known temperature of 1064.4°C.[17] It is at this time that the difference in the recorded thermocouple temperature and the gold point is precisely the thermal shunting error. As is illustrated in Fig. 10, the thermal arrest at the gold point lasted for approximately nine seconds, and with the temperature monitoring capability of CODAS, seventy-five temperature measurements were made over

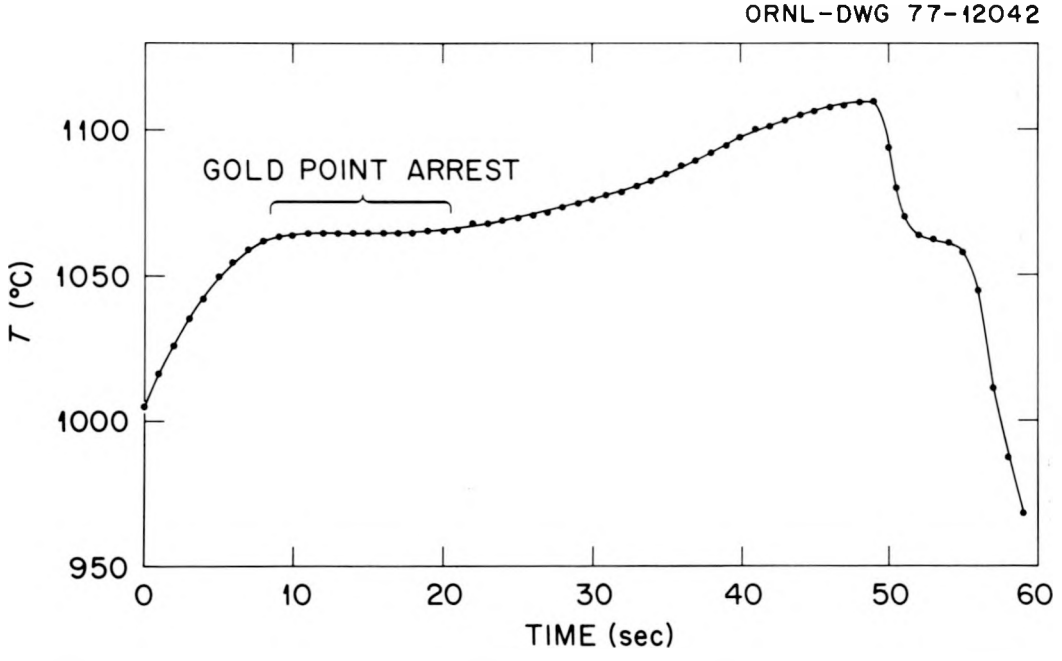

Fig. 10. Thermal Arrest Observed in Gold-Point Determination.

this time interval, the average temperature indicated by the thermocouple being 1064.4 ± 0.3°C. This rather remarkable result suggests that temperature measurements in the MiniZWOK apparatus are good and that previously estimated thermal shunting effects are experimentally determined to be negligible.

An additional test was made of this negligible shunting error result by measuring the α-γ phase transition temperature for an iron* specimen formed into the tube and specimen dimensions of the PWR tubing used in the steam oxidation studies. This experiment was of a similar nature to that of the gold melting point determination, but since the α-γ transition is a solid-solid transformation the thermocouples could be welded directly to the iron sample. The thermal arrest obtained on heating through the α-γ transformation point was 912.7 ± 0.1°C (1674.9 ± 0.2°F). While iron is by no means a standard reference material for temperature calibration the accepted value for α-γ transition temperature in high purity iron is 912°C (1674°F).[18]

These two experiments coupled with previously documented electrical shunting errors prove that no detectable thermal shunting errors occur in reporting measured temperatures in the MiniZWOK apparatus.

---

*Marz Iron obtained from Materials Research Corp. Vendor certified analysis (ppm by wt): 12 C, 60 O, 1.0 H, 10 N, <0.1 Al, 1.6 Na, 0.87 Mg, 0.70 P, 2.60 S, 0.80 Cl, 1.80 K, 0.80 Ca, 1.40 Ti, 0.60 Cu, <0.10 Si, 1.60 Cr, <0.10 Ni, 1.90 Zn, <0.10 Ga, <0.10 Zr, <0.10 Nb, <0.10 Mo, <0.10 Pd, <0.10 Ag, <0.10 In, <0.10 Sn, <0.10 Sb, <0.10 Ta, <0.10 Pt, <0.10 Au, <0.10 Pb, others <0.10.

REFERENCES

1. J. V. Cathcart, *Quarterly Progress Report on the Zirconium Metal-Water Oxidation Kinetics Program Sponsored by the NRC Division of Reactor Safety Research for April–June 1976*, ORNL/NUREG/TM-41 (August 1976).

2. *ibid.*, *October–December 1976*, ORNL/NUREG/TM-87 (February 1977).

3. *ibid.*, *January–March 1977*, ORNL/NUREG/TM-110 (May 1977).

4. *ibid.*, *July–September 1976*, ORNL/NUREG/TM-62 (December 1976).

5. S. Kawasaki, T. Furuta, and H. Hashimoto, *Reaction of Zircaloy Cladding with Steam under Simulated Loss-of-Coolant-Accident Conditions*, JAERI-M-6181 (July 1975).

6. S. Leistikow, H. v. Berg, and D. Jennert, "Comparative Studies of Zircaloy-4/High Temperature Steam Oxidation under Isothermal and Temperature Transient Conditions," in *Proceedings, CSNT Specialist Meeting on the Behavior of Water Reactor Fuel Elements under Accident Conditions*, Spatind, Nord-Torpa, Norway, September 13–16, 1976, in press.

7. R. F. Mattas and H. K. Brimbaum, "Isotopic Effects on the Motion of O-H Clusters in Nb," *Acta Met.* 23: 973–77 (1975).

8. C. Baker and H. K. Birnbaum, "Anelastic Studies of Hydrogen Diffusion in Niobium," *Acta Met.* 21: 865–72 (1973).

9. C. Roy, "An Experiment to Clarify the Effect of Dissolved Oxygen on the Therminal Solubility of Hydrogen in Zirconium," *J. Nucl. Mater.* 13: 275–7 (1964).

10. P. Kofstad, *Nonstoichiometry, Diffusion and Electrical Conductivity in Binary Metal Oxides*, Wiley-Interscience, New York, N.Y., 1972, pp. 152–165.

11. L. A. McClaine and C. P. Coppel, "Electrical Conductivity Studies of Tetragonal Zirconia," *J. Electrochem. Soc.* 113: 80–85 (1966).

12. B. Cox, "Oxidation of Zirconium and Its Alloys," *Advances in Corrosion Science and Technology*, Vol. 5, M. G. Fontana and R. M. Staehle, Eds., Plenum Press, N.Y., 1976, pp. 173–391.

13. K. Hauffe and V. Martinez, "Oxidation and Corrosion of Tin-Coated Zircaloy-4," *J. Electrochem. Soc.* 123: 595–602 (1976).

14. G. J. Yurek, J. V. Cathcart, and R. E. Pawel, "Microstructures of the Scales Formed on Zircaloy-4 in Steam at Elevated Temperatures," *Oxidation of Metals* 10: 255–76 (1976).

15. R. E. Pawel, *Zirconium Metal-Water Oxidation Kinetics III. Oxygen Diffusion in Oxide and Alpha Zircaloy Phases*, ORNL/NUREG-5 (October 1976).

16. J. V. Cathcart, D. L. McElroy, R. E. Pawel, R. A. Perkins, R. K. Williams, and G. J. Yurek, *Zirconium Metal-Water Oxidation Kinetics I. Thermometry*, ORNL-5102 (February 1976).

17. "The International Practical Temperature Scales of 1968," (adopted by the Comité International des Poids et Mesures), *Metrologia* 5(2): 35–44 (1969).

18. C. J. Boulanger, *Revue de Metallurgie* 53: 312 (1956).

ORNL/NUREG/TM-132
Dist. Category NRC-3

INTERNAL DISTRIBUTION

1. C. K. Bayne
2. M. Bender
3. J. R. Buchanan
4. J. J. Campbell
5. K. R. Carr
6—31. J. V. Cathcart
32. R. H. Chapman
33. W. B. Cottrell
34. F. L. Culler
35. D. G. Davis
36. R. E. Druschel
37. G. G. Fee
38. D. E. Ferguson
39. J. H. Freels
40. J. A. Hawk
41. R. A. Hedrick
42—44. M. R. Hill
45. D. O. Hobson
46. G. Hoffman
47. S. H. Jury
48. T. G. Kollie
49. B. C. Leslie
50. T. S. Lundy
51. F. C. Maienschein
52. D. L. McElroy
53. C. J. McHargue
54. R. A. McKee
55. C. S. Meadors
56. F. H. Neill
57. R. E. Pawel
58. R. A. Perkins
59. H. Postma
60. E. T. Rose
61. R. L. Shipp
62. D. B. Trauger
63. J. R. Weir
64. R. K. Williams
65. Patent Office
66—67. Central Research Library
68. Document Reference Section
69—73. Laboratory Records Department
74. Laboratory Records (RC)

EXTERNAL DISTRIBUTION

75—79. Director, Division of Reactor Safety Research, Nuclear Regulatory Commission, Washington, DC 20545
80. Director, Reactor Division, ERDA, ORO
81. Director, Research and Technical Support Division, ERDA, ORO
82—84. R. F. Fraley, ACRS
85. M. Levenson, Electric Power Research Institute, 3412 Hillview Avenue, P.O. Box 10412, Palo Alto, CA 94305
86—87. W. Loewenstein, Electric Power Research Institute, 3412 Hillview Avenue, P.O. Box 10412, Palo Alto, CA 94305
88. H. Seipel, Der Bundesminister fur Forschung and Technologie, 53 Bonn 12, Postfach 120370, Federal Republic of Germany
89—408. Given distribution as shown in NRC category 3 (25 copies — NTIS)

☆ U.S. GOVERNMENT PRINTING OFFICE: 1977-748-189/178